Journal of Power Sources, 7 (1981/82) 65 - 72

PLASTIC-BONDED ELECTRODES FOR NICKEL–CADMIUM ACCUMULATORS. VI. OXYGEN RECOMBINATION RATE ON SEALED CELL CADMIUM ELECTRODES

J. MRHA, J. JINDRA, M. MUSILOVÁ, J. PEIZKER and M. POLYDOROVÁ

J. Heyrovský Institute of Physical Chemistry and Electrochemistry, Czechoslovak Academy of Sciences, 102 00 Prague 10 (Czechoslovakia)

J. GARCHE and M. HAUPTMANN

Technical University of Dresden, Chemical Division, 8027 Dresden (G.D.R.)

(Received October 27, 1980; in revised form January 24, 1981)

Summary

The recombination (*i.e.*, reduction) of oxygen on pocket-type cadmium electrodes, utilizable in sealed Ni–Cd cells, occurs on areas covered with a thin layer of alkaline electrolyte. Hence, in the presence of a non-woven electrolyte carrier with a low permeability for oxygen, or by blocking the side of the electrode facing the gas space of the cell (which is not in contact with the electrolyte carrier), the recombination of oxygen is reduced to an insignificant level for sealed Ni–Cd cells. A comparison of results obtained with pocket-type and plastic-bonded cadmium electrodes showed that oxygen is reduced on metal parts of the electrode (perforated pocket, current collector, contacting metal screen) which are covered with a thin electrolyte layer, are easily accessible to oxygen, and are short-circuited by the electroactive Cd/Cd^{2+} material. The latter has a sufficiently negative potential and electronic conductance to allow the electroreduction of oxygen to take place.

Introduction

The widespread use of sealed Ni–Cd cells is the result of research going back to the beginning of this century when attempts were first made to seal the alkaline Ni–Fe system on the basis of the direct H_2 and O_2 recombination reaction in the later stage of charging [1]. It became clear by the thirties that the most promising solution for a sealed secondary system of commercial importance consisted of consuming the oxygen formed on the positive electrode directly by the negative electrode. The first relevant studies, however, did not reveal clearly the principle of oxygen recombination [2, 3]; this occurred later [4] when the first sealed Ni–Cd cells operated

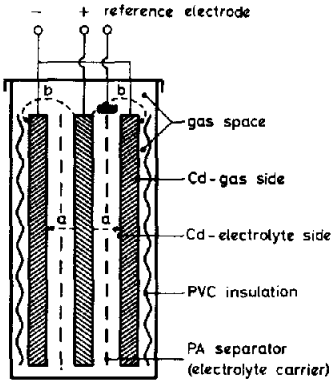

Fig. 1. Schematic diagram of the test cell. Arrow a — "inner mechanism", arrow b — "outer mechanism".

on this principle were patented [5]. Extensive use of these cells was, however, not possible until a suitable separator, functioning as an electrolyte carrier, was developed [6] which allowed transport of oxygen from the positive to the negative electrode. Sealed Ni–Cd cells of the button, cylindrical, or prismatic type are manufactured nowadays and their electrodes are either pressed (with an envelope made from a perforated metal sheet or a metal screen) or sintered (the electroactive material is in the pores of a sintered metal skeleton).

Research work has continued since the manufacture of sealed Ni–Cd cells began, and much effort has been expended in studying the mechanism of oxygen recombination on the cadmium electrode [7 - 10]. This was shown to proceed even in the absence of cadmium on the sintered nickel support [7]; the reaction is first order with respect to oxygen pressure [8] and is controlled by oxygen diffusion [8, 9]. Attempts to determine whether, in the presence of cadmium, a chemical mechanism according to the reaction

$$2Cd + O_2 + 2H_2O \rightleftharpoons 2Cd(OH)_2$$

was occurring or an electrochemical mechanism according to

$$O_2 + 2H_2O + 4e^- \rightleftharpoons 4OH^-$$

were unsuccessful, since the fundamental initial step is an electron transfer reaction in both instances [11]. If the oxygen reduction is followed by desorption of OH^- ions, then the mechanism can be described as electrochemical, whereas if the ions react immediately with Cd^{2+} obtained by the reaction

$$Cd \rightleftharpoons Cd^{2+} + 2e^-$$

with the formation of $Cd(OH)_2$, the mechanism can be conventionally described as chemical [11].

With regard to the construction of sealed Ni–Cd cells, it is important to determine on which part of the cadmium electrode the recombination of oxygen takes place. There are two possible choices (see Fig. 1): the electrolyte side of the electrode, which is in contact with the separator functioning as electrolyte carrier, or the gas side, which is placed in the gas space of the accumulator. The evolved oxygen either passes from the positive electrode, through the separator (electrolyte carrier), to the negative electrode ("inner mechanism" — arrow a), or escapes into the gas space and thence to the gas side of the cadmium electrode ("outer mechanism" — arrow b). It has not been determined to date which of these systems is occurring. This problem, together with the study of the mechanism of recombination, is the subject of the present work.

Experimental

Electrodes

The positive electrodes were commercial pocket electrodes for prismatic, sealed Ni–Cd cells of dimensions 45 × 75 mm. Their capacity at the 5 h discharge rate was 2 - 2.2 A h. The negative electrodes were pocket or plastic-bonded cadmium (PB-Cd) electrodes. The former were those used in prismatic, sealed Ni–Cd cells with dimensions of 45 × 75 mm. Their capacity at the 5 h discharge rate was 2.5 - 3 A h. The PB-Cd electrodes contained an active material used in commercial pressed electrodes for sealed Ni–Cd cells (essentially powdered Cd with a surface oxide film formed in the course of drying). This active material was blended with 5 wt.% PTFE (Fluon CD-1, ICI, Great Britain). The electrode dimensions were 40 × 75 mm, and their capacity was 2.5 - 3 A h at the 5 h discharge rate. The preparation of the electrode with a net type current collector, F 0.8 (wire diameter 0.8 mm), electroplated with nickel, has been described earlier [12, 13].

Separator and electrolyte carrier

The separator, at the same time the electrolyte carrier, was either one layer of woven polyamide fabric (thickness 0.25 mm, square density 124 g/m^2) or two layers of non-woven polyamide fabric (thickness 0.08 mm, square density 50 g/m^2).

Test cells

The test cells were assembled from one positive electrode wrapped in the polyamide fabric, placed between two cadmium electrodes, and inserted into a steel casing insulated from the electrodes by a layer of poly(vinyl-chloride) (PVC). A small Hg/HgO reference electrode (pressed mixture of HgO and graphite in a fine nickel gauze wrapped in polyamide separator and partly reduced to Hg) was placed close to the electrodes, forming a three-electrode system. After filling with a KOH solution of density 1.3 g/cm^3, the cells were set aside for 60 - 70 h with access to air. The free electrolyte was

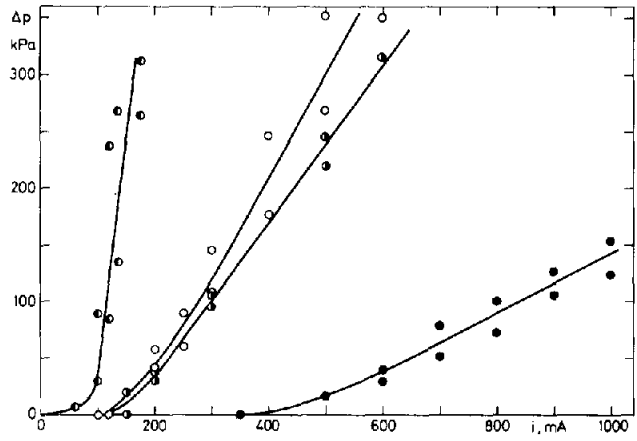

Fig. 2. Influence of the charging current on the steady state oxygen overpressure for pocket type cadmium electrodes with different materials in contact with their surfaces. ●, woven electrolyte carrier; ○, woven electrolyte carrier and PTFE blocking layer; ◐, non-woven electrolyte carrier and PTFE blocking layer; ◑, non-woven electrolyte carrier.

then removed by compressed air and the cells hermetically sealed with Plexiglass lids provided with openings for the current leads. Each cell was connected to a manometer having a range of 0 - 400 kPa following which it was placed in a thermostatted oil bath at 25 °C. This allowed the cell seals to be checked at the same time.

Electrochemical measurements

Each cell was cycled at a charging current ranging from 60 to 1000 mA until a steady overpressure was attained (after 16 - 30 h). The discharge was at the 5 h rate to a cut-off of zero volts. We followed the dependence of overpressure, Δp, on the charging current, i, in the steady state, and the dependence of the rate of fall of overpressure, after switching off the charging current, on the value of Δp at which the current was interrupted. The latter dependence was determined from the slope of the plot of Δp against time over a period of about 30 min. Some cells were subjected to long-term overcharge tests (140 h at 600 mA).

Results and discussion

Pocket cadmium electrodes with different modifications to the gas and electrolyte sides

The dependences of the steady value of Δp on the charging current for different pocket type cadmium electrodes are shown in Fig. 2; they can be divided into the following three groups according to decreasing rate of recombination:

(1) electrodes with woven electrolyte carrier and untreated gas side (only corrugated and perforated PVC insulation was applied);

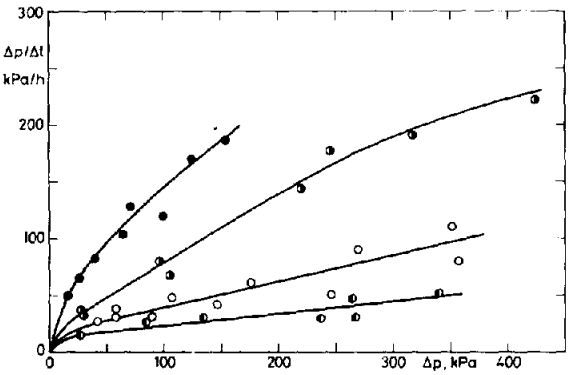

Fig. 3. Influence of the steady state oxygen overpressure on the rate of overpressure drop from the same electrodes as in Fig. 2.

(2) electrodes with non-woven electrolyte carrier and untreated gas side and electrodes with woven electrolyte carrier and a contacting layer of PTFE blocking the transport of oxygen to the gas side;

(3) electrodes with non-woven electrolyte carrier and a contacting layer of PTFE blocking the transport of oxygen to the gas side.

It is seen from Fig. 2 that the reduction of oxygen takes place in the final stage of charging, or during overcharging, on those parts of the pocket cadmium electrode which are covered with a thin electrolyte film. This film is most extensive on electrodes combined with a woven electrolyte carrier and corrugated and perforated PVC insulation on the gas side (group 1), hence, these electrodes show the highest recombination rate. The ratio between the recombination rates on the gas ("outer mechanism") and electrolyte ("inner mechanism") sides of the cadmium electrode depends on the conditions of existence of the electrolyte film on the gas and electrolyte sides of the electrode (porosity, thickness, etc., of the electrolyte carrier and of the corrugated and perforated PVC insulation).

When the gas side is blocked with a compact layer (PTFE) or the electrolyte side is in contact with two layers of non-woven electrolyte carrier, the recombination rate of oxygen decreases considerably (group 2), since the formation of an electrolyte film is hindered.

In the case of a simultaneous blocking of the gas side of the electrode and use of an electrolyte carrier with a low permeability for oxygen (group 3), the recombination of oxygen is almost completely hindered and takes place almost entirely on the metal parts that are accessible to oxygen (edges, plate tabs, etc.).

A similar behaviour is seen from the dependences of the rate of fall of the overpressure after interrupting the charging current on the stationary overpressure, Δp, shown for the three groups of electrodes in Fig. 3. The cadmium electrodes with the free gas side and woven electrolyte carrier again show the highest recombination rate.

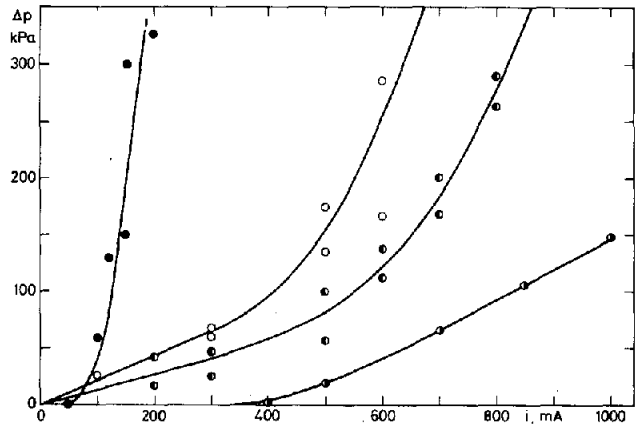

Fig. 4. Influence of the charging current on steady state oxygen overpressure for PB-Cd electrodes with different metal nets on the gas side. ●, without net; ○, F 0.4 net; ◐, 2 × F 0.18 net; ◑, pocket type electrode (for comparison).

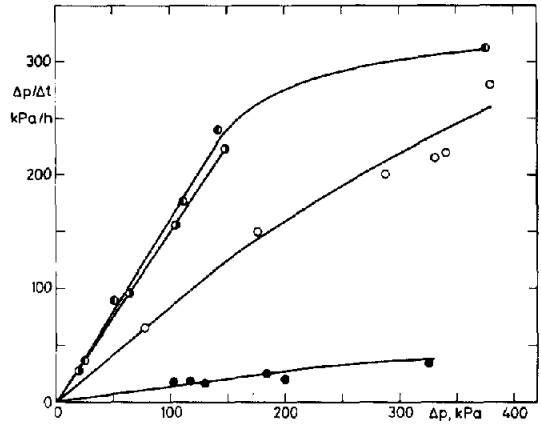

Fig. 5. Influence of the steady state oxygen overpressure on the rate of overpressure drop for the same electrodes as in Fig. 4.

It may be concluded that with pocket plate-type cadmium electrodes recombination of oxygen takes place to an extent applicable to sealed cells on those parts of the electrode which are covered by a thin film of electrolyte. A non-woven electrolyte carrier or a blocked gas side hinder the formation of this film. The ratio of oxygen recombination rates on the gas and electrolyte sides of the electrode is controlled only by the extent of the electrolyte film on them.

PB-cadmium electrodes with modified gas side

The results for PB-Cd electrodes with various modifications to the gas sides are shown in Figs. 4 and 5. The gas sides of some electrodes were either in contact with a corrugated and perforated PVC insulation or with either of

TABLE 1

Characteristics of the nets

Net type	Wire diam. (mm)	Mesh size (mm)	Square density (kg/m^2)
F 0.18	0.18	0.71	0.457
F 0.4	0.4	1.0	1.48

TABLE 2

Overpressure values after long-term overcharging for different types of cadmium electrode

Electrode type	Gas side	Electrolyte side	Overpressure after 140 h overcharging at 0.6 A (kPa)
Pocket	free	woven fabric	60 - 69
Pocket	blocked with PTFE	woven fabric	> 400
Pocket	free	non-woven fabric	~350
PB-Cd	free	woven fabric	>400
PB-Cd	2 x F 0.18	woven fabric	117 - 192
PB-Cd	1 x F 0.4	woven fabric	257 - 332

two types of nickel-plated steel nets (Table 1). It is seen that the recombination rate of oxygen on electrodes without a metal net is the same as that on pocket electrodes with blocked oxygen transport (with an insulator foil on the gas side or a non-woven electrolyte carrier on the electrolyte side). Hence, the PB-Cd electrode under study was unable to reduce oxygen in spite of its easy access to the gas or electrolyte sides of the electrode. The active mass, which was of the same type as that in pocket electrodes, did not catalyse the reduction of oxygen at a sufficient rate. This is in accord with the results of measurements on pure Cd electrodes, where the reduction of oxygen was hindered by an oxide film [14]. In our case, the reduction of oxygen obviously takes place mainly on the metal parts of the cadmium electrode which are covered with an electrolyte film and are short circuited by the electroactive material, ensuring a sufficiently negative potential. The current collector of the PB-Cd electrode is unsuitable for this purpose since it is placed in the interior of the active layer and is not easily accessible to oxygen.

If one or more metal nets are in short circuit with the gas side of the PB-Cd electrode and are covered with an electrolyte film, the rate of oxygen reduction increases and is roughly proportional to the geometric surface area of the net.

The results shown in Figs. 4 and 5 suggest that the recombination of oxygen proceeds by an electrochemical mechanism, similar to that of oxygen

electrodes in fuel cells. The oxygen electrode represented by a metal net covered with an electrolyte film and short-circuited by the cadmium electrode has a sufficiently negative potential to permit the reduction of oxygen at a sufficient rate. Thus, PB-Cd electrodes in contact with an added net are suitable for commercial sealed Ni–Cd accumulators.

The resulting overpressures in test cells after long-term overcharging (0.6 A for about 140 h), for electrodes of different construction, are given in Table 2. They are in accord with the results shown in Figs. 1 - 4 for shorter periods of overcharging.

The influence of the contacting net material and of additives in the active material will be studied in further work.

Conclusions

The reduction (recombination) of oxygen in sealed Ni–Cd cells takes place mainly on those metal parts of the Cd electrode which are in short circuit with its active layer, are covered with an electrolyte film, and are easily accessible to oxygen. The recombination rate can be adjusted within wide limits by modifying the gas side of the cadmium electrode (by using a metal net, a perforated pocket or an insulating layer), as well as by the type of the electrolyte carrier (woven or non-woven fabric). The mechanism of the reduction is electrochemical (similar to alkaline oxygen electrodes) and the necessary negative potential is maintained by the Cd/Cd^{2+} system.

References

1 T. A. Edison, *US Pat. 1,016,874* (1912).
2 A. E. Lange, E. Languth, E. Breuning and A. Dassler, *Ger. Pat., 674,829* (1933); *US Pat. 2,131,592* (1938).
3 G. F. Rublee, *US Pat. 2,269,040* (1939).
4 A. Levin and W. S. Thompson, *Brit. Pat. 571,820* (1943).
5 G. Neumann and U. Gottesmann, *US Pat. 2,571,927* (1951).
6 R. Jeannin, *French Pat. 102,709* (1950).
7 E. G. Baars, *Proc. 12th Annu. Battery Research and Development Conf., Fort Monmouth, 1958*, p. 25.
8 K. Dehmelt and H. von Döhren, *Proc. 13th Annu. Battery Research and Development Conf., Fort Monmouth, 1959*, p. 85.
9 U. B. Thomas, in D. H. Collins (ed.), *Batteries*, Pergamon Press, Oxford, 1963, p. 117.
10 H. B. Lunn and J. Parker, in D. H. Collins (ed.), *Batteries 2*, Pergamon Press, Oxford, 1964, p. 129.
11 P. Rüetschi and I. B. Ockermann, *Electrochem. Technol., 4* (1966) 383.
12 J. Jindra, M. Mrha, K. Micka, Z. Zábranský, B. Braunstein, J. Malík and V. Koudelka, in D. H. Collins (ed.), *Power Sources 6*, Academic Press, London, New York, San Francisco, 1977, p. 181.
13 J. Jindra, J. Mrha,K. Micka, Z. Zábranský, V. Koudelka and J. Malík, *J. Power Sources, 4* (1979) 227.
14 G. I. Avilova, B. N. Afanasiev, N. A. Borisova, Z. A. Timofeeva and N. N. Milyutin, *Zh. Prikl. Khim., 51* (1978) 698.

Journal of Power Sources, 7 (1981/82) 73 - 82

DISCHARGE BEHAVIOUR OF ELECTRODEPOSITED PbO_2 AND Pb ELECTRODES

KENJI ASAI, MASAHARU TSUBOTA, KUNIO YONEZU and KOJI ANDO

Lead–Acid Battery Laboratory, Corporate R & D Centre, Japan Storage Battery Co., Ltd., Kyoto (Japan)

(Received February 7, 1981)

Summary

The discharge behaviour of electrodeposited lead dioxide and lead electrodes was investigated under various conditions; the surfaces of the discharged electrodes were observed with a scanning electron microscope. Both the positive and negative electrodes were passivated by a covering of deposited lead sulphate crystals. The amount of lead sulphate required for passivation depended on the size of the crystals.

Introduction

During discharge, both the positive and negative active materials of lead–acid batteries are converted to resistive, solid lead sulphate. Therefore, the discharge capacity will be affected by the morphology and deposition mode of the $PbSO_4$ crystals. It is well-known that the capacity of lead–acid battery plates is influenced by geometrical factors such as plate thickness [1, 2], porosity [1], specific surface area [1], etc., and also by the discharge conditions such as discharge current [1 - 4] and concentration [2, 5, 6] and temperature [2, 4] of the sulphuric acid.

In order to improve the discharge performance of the plates, it is necessary to clarify the mechanisms which restrict the discharge reactions.

In this study we have investigated the influence of discharge current density, electrolyte concentration and temperature on the discharge capacity of non-porous PbO_2 and Pb electrodes prepared by electrodeposition. Further, the morphology of $PbSO_4$ crystals deposited on the electrode surface after discharge was observed with a scanning electron microscope (SEM).

Experimental

Preparation of electrodes

Lead dioxide electrodes were prepared by electrodeposition of β-PbO_2 on smooth platinum plates of 8 cm^2 surface area from lead nitrate solution.

Plating was carried out at a current density of 50 mA/cm^2 and at a temperature of 30 °C for 5 min. The plating solution consisted of 350 g/liter $Pb(NO_3)_2$ and 25 g/liter $Cu(NO_3)_2$. The thickness of the electrodeposited PbO_2 layer was about 15 μm.

Lead electrodes were prepared by electrodeposition of Pb on mechanically polished, pure lead plates of 2.25 cm^2 surface area from lead borofluoride solution. Plating was carried out at a current density of 100 mA/cm^2 for 5 min at 25 °C. The plating solution consisted of 336 g/liter HF, 315 g/liter H_3BO_3 and 450 g/liter $2PbCO_3 \cdot Pb(OH)_2$. The thickness of the electrodeposited Pb layer was about 30 μm.

Figure 1 shows the surfaces of the electrodeposited PbO_2 and Pb electrodes. The surfaces were non-porous, although some cracks were observed. In these electrodes, the discharge reaction took place almost uniformly over the whole surface.

Discharge test

The electrodeposited PbO_2 and Pb electrodes were discharged at various current densities until a rapid potential change took place. Hg/Hg_2SO_4(1N-H_2SO_4) or $PbO_2/PbSO_4$ couples were used as reference electrodes. To eliminate oxide film, Pb electrodes were reduced cathodically at 0.1 mA/cm^2 for about 4 min prior to discharge. A large excess of electrolyte was used so that the concentration changed little during discharge.

During and after discharge, the electrodes were withdrawn, washed with deoxygenated water, and dried in a vacuum oven. SEM observations were carried out on the surface and/or the cross-section of the electrodes after gold shadowing.

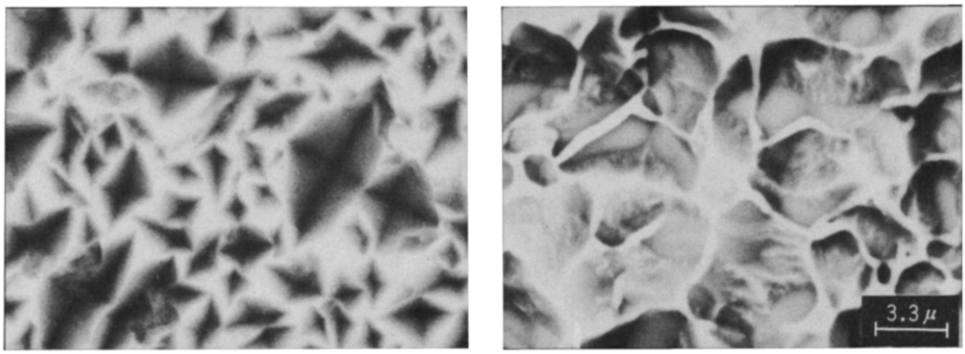

(a) (b)

Fig. 1. Surface of test electrodes. (a) Electrodeposited PbO_2 electrode; (b) electrodeposited Pb electrode.

Results and discussion

Discharge capacity

The relations between the discharge current density and the discharge duration time of the PbO_2 and Pb electrodes are shown in Fig. 2. For both

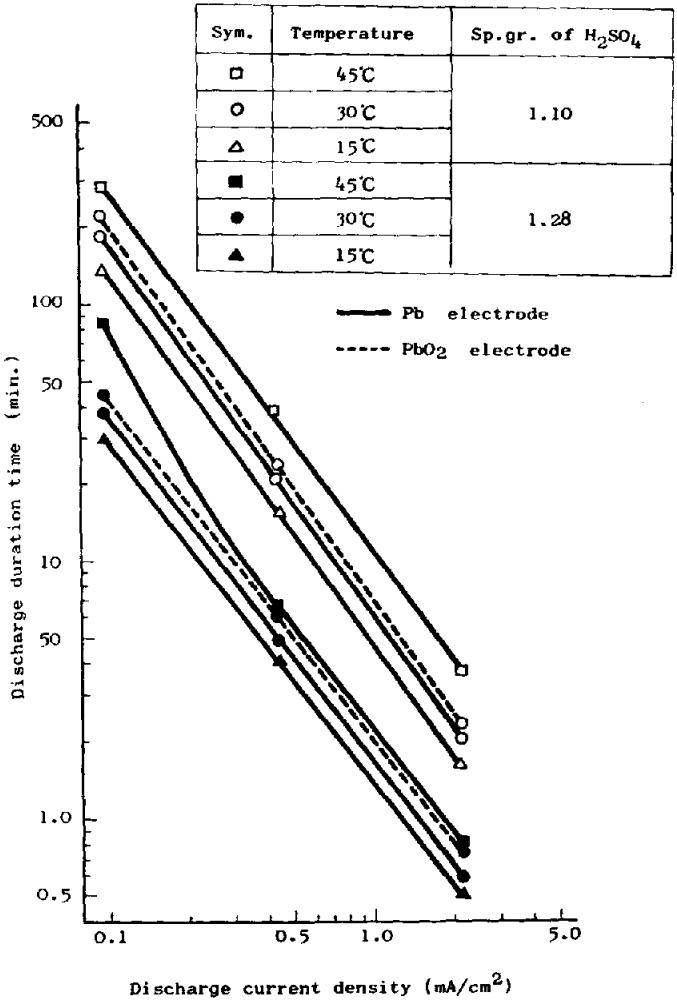

Fig. 2. Dependence of discharge duration time of electrodeposited Pb and PbO_2 electrodes on discharge current density.

the PbO_2 and Pb electrodes, the capacity decreased similarly with increasing current density. For these electrodeposited electrodes, as well as for conventional lead–acid battery plates, it will be noted that Peukert's equation, $I^n \times t = C$, for the relation between current density, I, and duration time, t, where n and C are constants can be generally applied. The values of constant n calculated from Fig. 2 are in the range 1.34 - 1.46 for both electrodes, and these values are approximately the same as those for pasted type positive or negative plates [4].

Figure 3 shows the dependence of discharge capacity on the electrolyte concentration for the electrodeposited electrodes. For both PbO_2 and Pb electrodes, as the concentration of sulphuric acid increased, the discharge

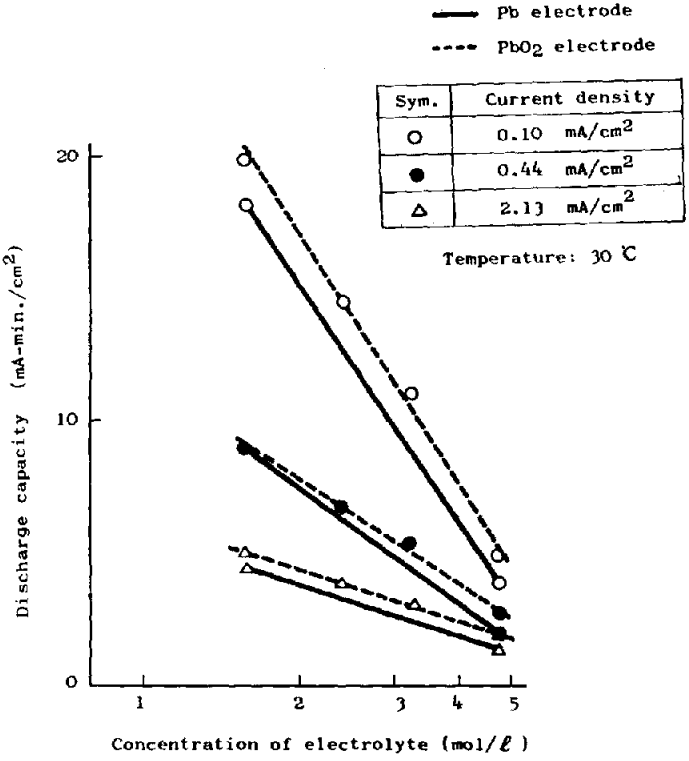

Fig. 3. Relationship between discharge capacity and electrolyte concentration for electrodeposited Pb and PbO_2 electrodes.

capacity decreased. This result is in opposition to that of actual lead–acid battery plates with porous structures where the discharge capacity increases generally as the concentration of acid increases. The difference in electrolyte concentration effect may be attributable to the difference in the electrode structure, such as porosity, pore size distribution, specific surface area, etc.

The relations between the temperature and the capacity of the electrodes are shown in Fig. 4. The discharge capacity increased with temperature rise. The influence of temperature on the capacity was particularly noticeable in dilute electrolyte.

It is apparent from these results that the relations between the discharge conditions and the capacity for both PbO_2 and Pb electrodes are almost the same. The capacity of the electrodes decreases with increasing current density, and electrolyte concentration and lower electrolyte temperature.

Morphology of $PbSO_4$ crystals deposited during discharge

Figures 5 and 6 show the morphology of $PbSO_4$ crystals deposited on the surfaces of PbO_2 and Pb electrodes after complete discharge under various conditions of current density, concentration, and temperature.

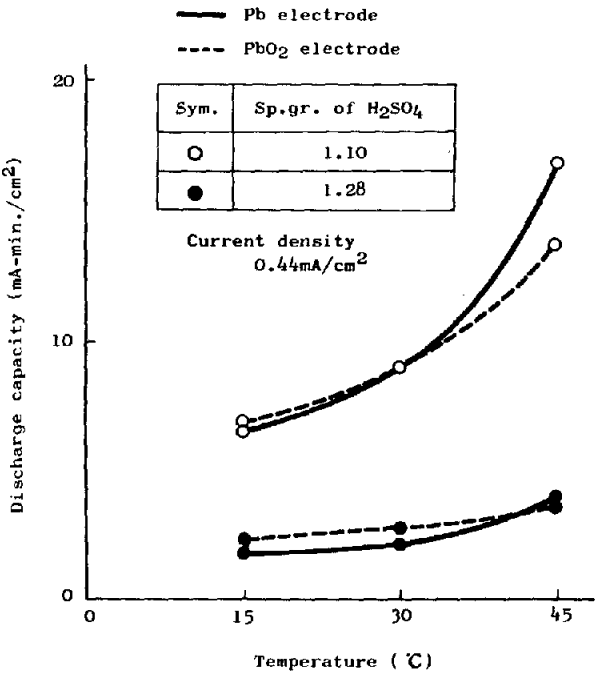

Fig. 4. Relationship between discharge capacity and temperature for electrodeposited Pb and PbO_2 electrodes.

Figure 5 shows the effect of current density on the morphology of $PbSO_4$ in electrolytes of 1.10 and 1.28 sp. gr., and Fig. 6 shows the effect of temperature at the same sulphuric acid concentrations. It can be seen that the $PbSO_4$ crystals deposited on both PbO_2 and Pb electrodes become larger with decreasing current density, and with rising temperature and lower specific gravity of sulphuric acid. The $PbSO_4$ crystals deposited on PbO_2 electrodes had a prismatic form; whereas the crystals on Pb electrodes showed a dendritic structure in some cases. The difference in the $PbSO_4$ morphology suggests that the growth mechanism of the $PbSO_4$ crystals on each electrode differs, and the Pb electrodes are likely to develop an excessive supersaturation of Pb^{2+} ions during discharge.

Figure 7 shows typical cross-sections of the discharged electrodes. It can be seen from the Figure that the surfaces of the PbO_2 electrodes have been covered by a monolayer of $PbSO_4$ crystals, not by a multilayer of overlapping $PbSO_4$ crystals.

From the above observations, it may be suggested that the discharge is limited by complete coverage of the electrode surface with $PbSO_4$ crystals. The size of the crystals will play an important role in the discharge capacity of the electrode. For example, if the size of the crystals increases, the total amount of $PbSO_4$ required to cover the electrode surface increases and, consequently, the discharge capacity should be increased.

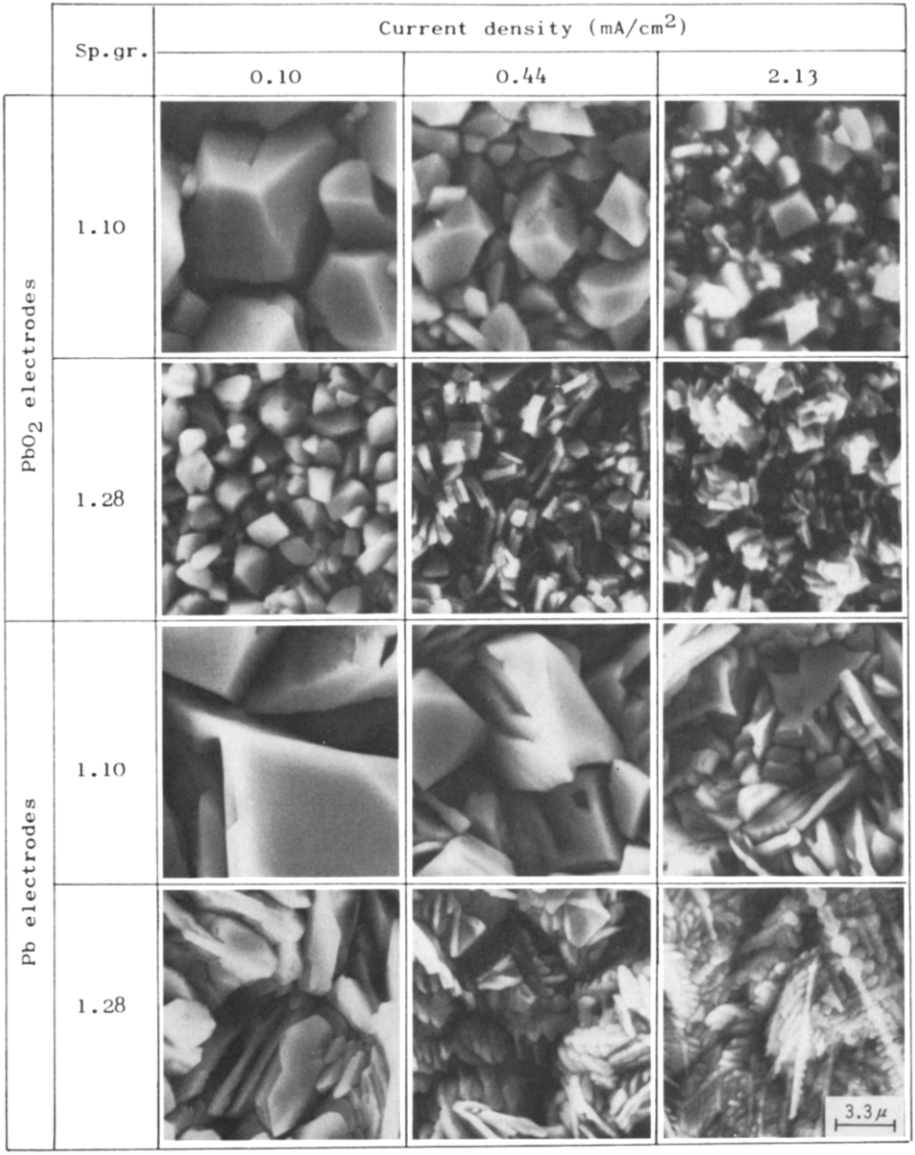

Fig. 5. Surface of electrodes after complete discharge at 30 °C.

Figure 8 shows how the $PbSO_4$ crystals cover the surface of the Pb electrode as discharge proceeds. In the initial stage (10% discharge of capacity), the $PbSO_4$ crystals which will become nuclei for deposition are scattered. As the discharge proceeds, $PbSO_4$ deposits around these crystals, and colonies of $PbSO_4$ crystals are formed (50% discharge). The colonies spread over the electrode surface as discharge proceeds (75% discharge). Finally, the surface of the Pb electrode is completely covered by deposited

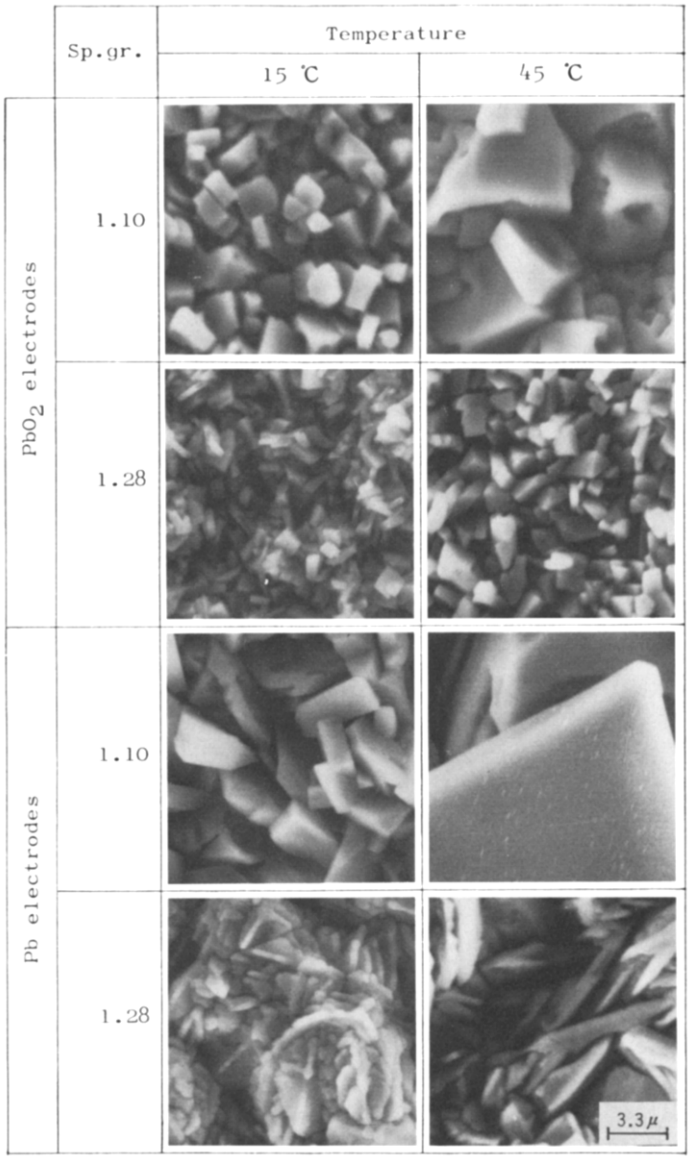

Fig. 6. Surface of electrodes after complete discharge at a current density of 0.44 mA/cm^2.

$PbSO_4$ crystals (100% discharge). Further, it can be seen that the size of the $PbSO_4$ crystals deposited during discharge is approximately constant and not affected by the state of discharge. The size of the deposited $PbSO_4$ crystals depends mainly on the discharge conditions, as shown earlier.

Effect of lignin on the size of the $PbSO_4$ crystals

The negative active material of a lead–acid battery usually contains an organic expander. In order to clarify the effect of the expander, the Pb and

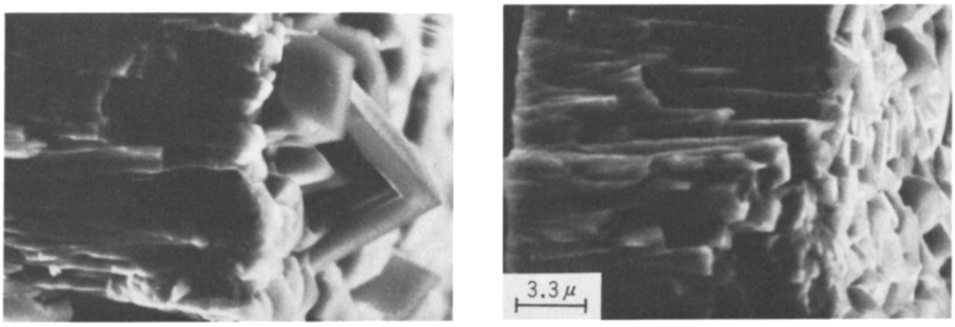

(a) (b)

Fig. 7. Sectional view of PbO_2 electrodes after complete discharge. Current density, 0.44 mA/cm^2; temperature, 30 °C. (a) Sp. gr. of electrolyte, 1.10; (b) sp. gr. of electrolyte, 1.28.

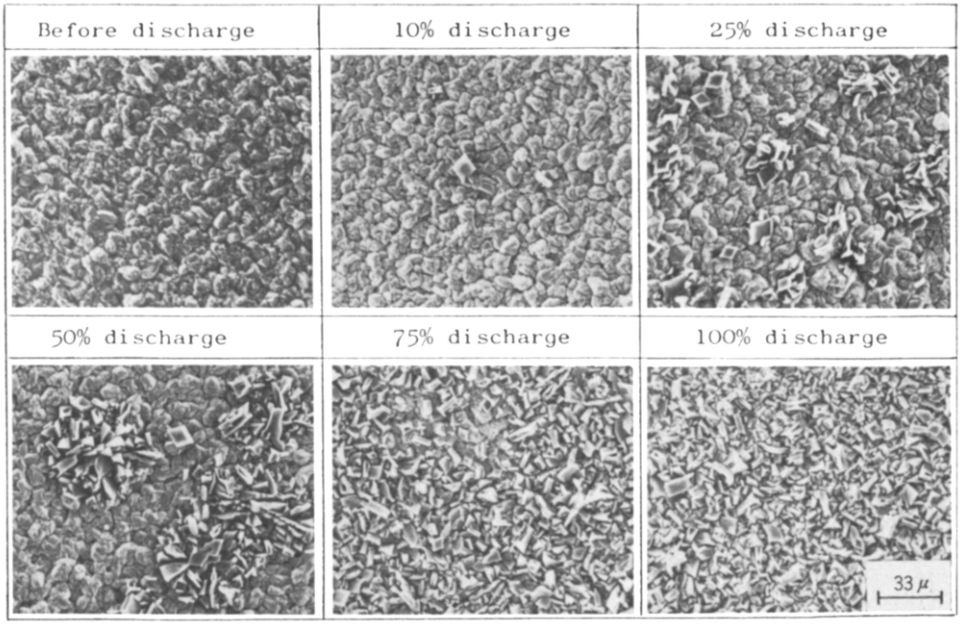

Fig. 8. Surface change of electrodeposited Pb electrode during discharge. Current density, 0.44 mA/cm^2; specific gravity, 1.10; temperature, 30 °C.

PbO_2 electrodes were discharged in electrolyte with lignosulphonate, and the discharge capacity and the morphology of the deposited $PbSO_4$ crystals were observed. One gram of the lignosulphonate was added to one liter of dilute sulphuric acid and the solution well stirred. The supernatant solution was used as electrolyte for the discharge test.

The discharge characteristics and the surfaces of the electrodes after discharge in the electrolyte with lignosulphonate are shown in Figs. 9 and 10, respectively. In the presence of lignin components in the electrolyte, the

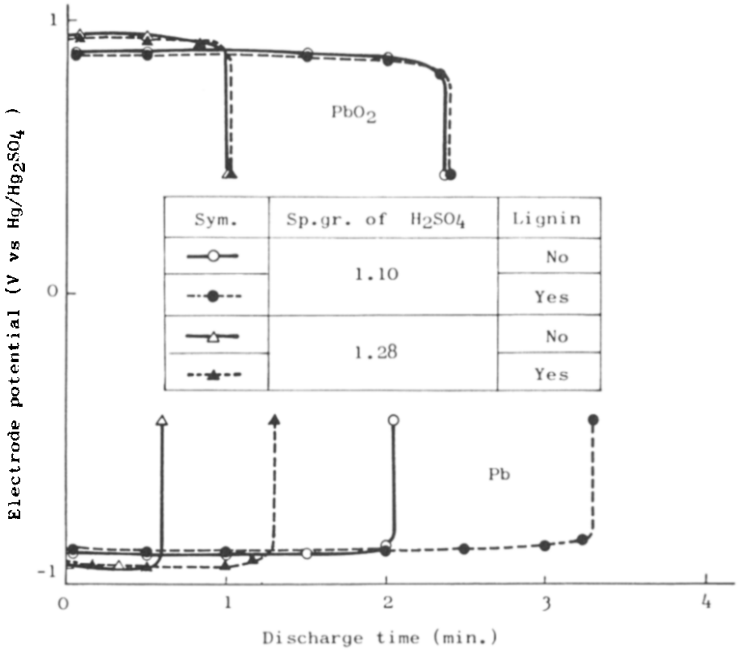

Fig. 9. Discharge characteristics of electrodeposited Pb and PbO_2 electrodes in the electrolyte with or without lignin. Current density, 2.13 mA/cm^2; temperature, 30 °C.

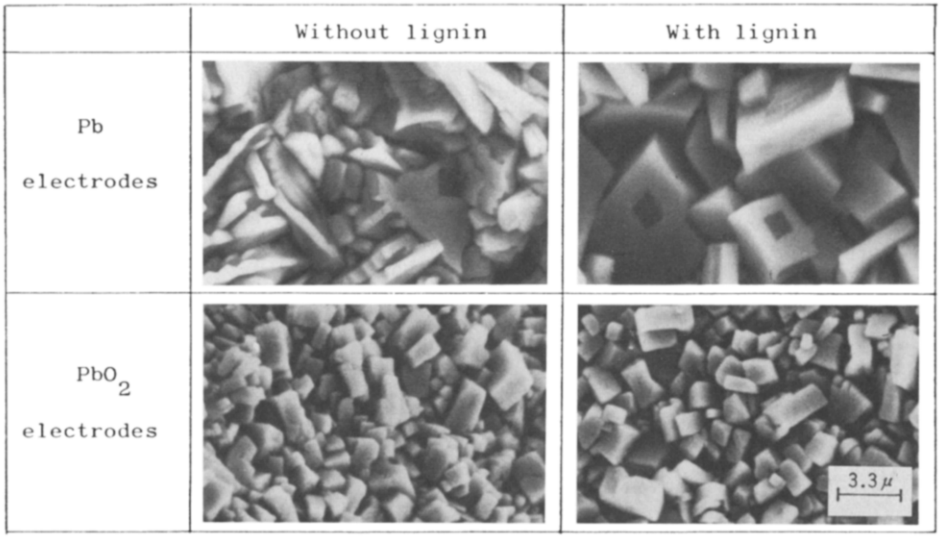

Fig. 10. Effect of lignin on $PbSO_4$ crystal size deposited on electrodeposited Pb and PbO_2 electrodes after complete discharge. Current density, 2.13 mA/cm^2; sp. gr., 1.10; temperature, 30 °C.

discharge duration time of the Pb electrodes increased remarkably, but the lignin had little effect on the duration time of the PbO_2 electrodes (Fig. 9). Furthermore, it can be seen that the size of the $PbSO_4$ crystals deposited on the Pb electrodes increases in the electrolyte containing lignin, but for the PbO_2 electrodes the presence of lignin scarcely affects the size of the crystals (Fig. 10). In this study, only the soluble component of lignosulphonate is contained in the electrolyte; the experimental conditions differ from the practical case where most of the organic expander is included in the negative active material in insoluble form. However, it is apparent that the $PbSO_4$ crystals deposited on the Pb electrodes become larger in the presence of lignin components and, consequently, the discharge capacity increases. This observation agrees with the result reported by Aguf *et al.* [7], where they pointed out that the action of lignin is to form coarse $PbSO_4$ crystals on the negative electrodes during discharge. It can be seen that the discharge reactions of both PbO_2 and Pb electrodes proceed *via* a solution–precipitation process; nevertheless, lignin has this remarkable affect on the Pb electrodes alone. This seems to be caused by the difference in the interaction between the electrodes and the lignin as an organic compound.

Conclusions

The discharge behaviour of electrodeposited PbO_2 and Pb electrodes with a non-porous structure was investigated under various discharge conditions, and the discharged electrodes were observed by SEM.

This study showed that the discharge capacity of both PbO_2 and Pb electrodes was equal to the amount of deposited $PbSO_4$ which completely covered the electrode surface. Also, the amount of $PbSO_4$ was defined by the crystal size. As the size of the crystals deposited during discharge became smaller, the discharge capacity decreased, because the electrode was passivated with a smaller amount of $PbSO_4$. With increasing discharge current density and concentration of sulphuric acid and with lower temperature, finer $PbSO_4$ crystals deposit on the electrode surface and cause a capacity decrease.

Furthermore, it was shown that in the presence of lignin in the electrolyte, the $PbSO_4$ crystals produced on the Pb electrode during discharge increased in size.

References

1 E. Voss and J. Freundlich, in D.H. Collins (ed.), *Batteries*, Pergamon Press, New York, 1963, p. 73.
2 G. Vinal, *Storage Batteries*, Wiley, New York, 4th Edn., 1955.
3 M. I. Gillibrand and G. R. Lomax, *Electrochim. Acta*, *8* (1963) 693.
4 P. E. Baikie, M. I. Gillibrand and K. Peters, *Electrochim. Acta*, *17* (1972) 839.
5 T. Chiku, *J. Electrochem. Soc. Jpn.*, *11* (1943) 17.
6 T. Ikeda, *J. Electrochem. Soc. Jpn.*, *13* (1944) 99.
7 I. A. Aguf, M. A. Dasoyan, L. A. Ivanenko, E. V. Parshikova and K. M. Soloveva, *Sov. Electrochem.*, *6* (1970) 1591.